An improved mechanistic model for predicting the molten core-concrete interaction process under severe accident

WEI Wei[1,2], QI Kelin[1], CAO Xinrong[2], CHEN Yanfang[1], and TAN Chao[1]

1 China Nuclear Power Operation Tech. Co., Ltd., Wuhan City 430223, China

2 Fundamental Science on Nuclear Safety and Simulation Technology Laboratory, Harbin Engineering University, Harbin City 150001, China

Abstract: To meet the domestic demand of software autonomous scheduling, an improved mechanistic model of the molten core-concrete interaction (MCCI) process under severe accidents has been developed. The Daya-Bay nuclear power plant is selected as the research object. The MCCI occurs under the station blackout (SBO) accident without the auxiliary feed water, and the large break loss of coolant (LBLOCA) accident without safety injection are calculated and analyzed. In order to verify the reasonableness and correctness of the new developed MCCI model, the calculation results of this model are compared with the large-scale analysis codes MAAP. The results indicate that the MCCI model of SIMSA code can simulate the MCCI process correctly and reasonably under multi-serial severe accidents.

Keywords: MCCI; SIMSA code; multi-serial severe accident; molten core-concrete interaction

1 Introduction

After the Fukushima severe nuclear accidents in Japan, national nuclear safety regulatory authorities of China have promoted the requirements for severe accident management of nuclear power plants, and the new version of the nuclear power plant operational safety requirements of China (HAF103) have been proposed that regulate nuclear power plant operators must accept severe accidents related training(NNSA, 2004). This requires that the FSS (full- scope simulator) of new plants should have severe accidents simulation capabilities, and the old ones should be updated to expand the simulation scope to the stage of severe accidents. Existing severe accidents analysis programs, such as MELCOR (Merrill *et al.*, 2010), MAAP4 (Ferng *et al.*, 2010), SCDAP-RELAP5 (Sharm *et al.*, 2011), CONTAIN (Carroll *et al.*, 1987), VICTORIA (Makynen *et al.*, 1997), CATHARE/ICARE (Bandini *et al.*, 2011), are too large scale and complex structure to be applied to the FSS.

In the hypothetical event of a severe accident in a pressurized water reactor (PWR), the fuel, cladding and structural elements will form corium in the reactor core. In some scenarios, corium is assumed to melt through the reactor pressure vessel and spread over the concrete basement of the reactor cavity. Molten core concrete interaction (MCCI) then occurs, which will lead to the concrete ablation (B. Tourniaire *et al.*, 2006).

Recently, a severe accident simulation code named Simulation code of Severe Accident(SimSA) (CNPO, 2014)in order to simulate the whole process in reactor severe accident condition is developed under the collaboration frame of CNPE (China Nuclear Power Engineering Corporation) and CNPO (China Nuclear Power Operation Corporation). The previous study indicates that this code can simulate both the thermo-hydraulic and the physic-chemical phenomena of the corium pool in interaction with a concrete basement (Wei Wei *et al.*, 2013).

In the present study, a mechanistic model of MCCI process under severe accidents is developed, and the hypothesized MCCI process basing on Daya-Bay

Received date: October 19, 2016
(Revised date: November 23, 2016)

nuclear power plant is selected as the research object. In addition, the analyzed results of the new developed model are compared with the large-scale analysis programs MAAP to verify the reasonableness and correctness. The calculation results show that a good agreement appears between the new model and MAAP programs. And the new developed model can simulate the MCCI process correctly and reasonably under multiple severe accident serials. In the next step, it will be applied to the FSS for severe accidents simulation.

In this paper, first a detail process model of MCCI will be introduction, and then the assessment process of this model will be done through comparing with MAAP code, at last related conclusion will be give about this MCCI model.

2 Modeling of the MCCI

Due to the heating of the molten core corium, the concrete firstly dehydrated and released water vapor, and then decomposed into water vapor and carbon dioxide, lastly melted into the corium group. Therefore, it is difficult to determine the structure of the molten corium group.

Generally, was assumed to be a hierarchical structure, its top is a lighter metal phase, and the lower is the heavier oxidation phase. This model ignores the chemical reaction between the metal phase and the oxide phase, and the possible inversion of hierarchical structure due to diluting of the oxide phase has not been considered too. Its structure is shown in Fig. 1.

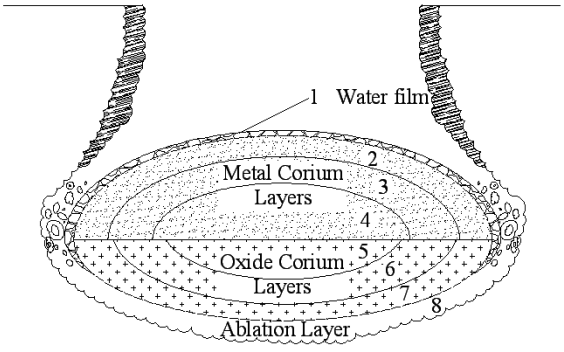

Fig. 1. The concrete base plate ablation package group diagram.

Where, the first layer is a water film, and from the second to fourth layers are metal layers (including: Zr and Fe), and from the fifth to seventh layers are oxide layers (including: UO2, ZrO2 and the oxide production of concrete ablation), and the eighth layer is concrete ablation zone.

2.1 Determine the initial state of ablation package group

In general, the molten corium from the failure pressure vessel contains four materials, which are UO2, Zr, ZrO2 and Fe. And the initial mass of each layers of the ablation package group can be calculated according to following equations:

$$\begin{cases} m_{APGi} = m_{H_2O}, i = 1 \\ m_{APGi} = \left(m_{Zr} + m_{Fe}\right)\beta_{APGi}, i = 2,3,4 \\ m_{APGi} = \left(m_{ZrO_2} + m_{UO_2}\right)\beta_{APGi}, i = 5,6,7 \end{cases} \quad (1)$$

When the initial average temperature of the corium is T_{ef} , then the actual temperature of component j can be described in following equations.

$$\begin{cases} T_{rej} = T_{ef}, T_{ef} < T_{meltj} \\ T_{rej} = T_{meltj}, T_{meltj} \le T_{ef} < T_{meltj} + T_{qmeltj} \\ T_{rej} = T_{ef} - T_{qmeltj}, T_{ef} \ge T_{meltj} + T_{qmeltj} \end{cases} \quad (2)$$

In which,

T_{meltj} is the melting point temperature of component j;

T_{qmeltj} is the corresponding temperature rise of the latent heat of phase change of component j.

Thus, the initial temperature in each layer is,

$$\begin{cases} T_{APGi} = T_{H_2O}, i = 1 \\ T_{APGi} = \sum_{j=1}^{4} T_{rej}\beta_{ij}, i = 2 \sim 7 \end{cases} \quad (3)$$

In which,

T_{H_2O} is the temperature of water film in first layer;

β_{ij} is the mass fraction of component j in the ith layer.

2.2 heat and mass transfer calculation in each layer

(1) heat and mass transfer calculation in the first layer

As referred previously, the first layer of the ablation package group is a water film on the molten metal. Therefore, the convective heat transfer coefficient between the first and the second layer is, [shown as Eq. (4)]

In which, ΔT_{21} is temperature difference between 2rd and 1st layer. The energy transmission between 2rd and 1st layer can be determined as follows, [shown as Eq. (5)]

In which, A_{APG1} is the area of the 1st layer, T_{av} is the average temperature of the reactor cavity.

Thus, the evaporation rate of the first layer can be calculated as follows, [shown as Eq. (6)]

And the temperature and mass of the 1st layer can be achieved, [shown as Eq. (7) and (8)]

$$\begin{cases} h_{21} = 34.5 P_{cont}^{\ 0.25} \Delta T_{21}^{\ 1.523}, \Delta T_{21} < 23.4 \\ h_{21} = 1.41\times 10^{7} P_{cont}^{\ 0.25} / \Delta T_{21}^{\ 2.575} + 0.4\sigma (T_{APG2}^{\ 4} - T_{APG1}^{\ 4}) / \Delta T_{21}, \Delta T_{21} \geq 23.4 \end{cases} \tag{4}$$

$$Q_{21} = \begin{cases} h_{21} A_{APG1} \Delta T_{21}, m_{APG1} > 0 \\ 0.4\sigma A_{APG1} (T_{APG2}^{\ 4} - T_{av}^{\ 4}), m_{APG1} = 0 \end{cases} \tag{5}$$

$$\begin{cases} F_{evap} = Q_{21} / (h_{evap} - h_{sat}), T_{APG1} \geq T_{sat} \\ F_{evap} = 0, T_{APG1} < T_{sat} \end{cases} \tag{6}$$

$$\begin{cases} T_{APG1} = T_{sat}, T_{APG1} \geq T_{sat} \\ T_{APG1} = \dfrac{T_{APG1} m_{APG1} c_{H_2O} + (Q_{21} + F_{inject} h_{inject} - F_{evap} h_{evap}) \Delta t}{m_{APG1} c_{H_2O}}, T_{APG1} < T_{sat} \end{cases} \tag{7}$$

$$m_{APG1} = m_{APG1} + (F_{inject} - F_{evap}) \Delta t \tag{8}$$

(2) Heat and mass transfer calculation in the metal layers

Base the hypotheses of the model, the 2nd, 3rd and 4th layers all are consisted of metal Fe and Zr. Thus the physical properties of the metal layers can be calculated with the following equation.

$$\begin{cases} m_{metal} = m_{Zr} + m_{Fe} \\ r_{metal} = \left(m_{Zr} r_{Zr} + m_{Fe} r_{Fe} \right) / m_{metal} \\ l_{metal} = 10 \left(m_{Zr} l_{Zr} + m_{Fe} l_{Fe} \right) / m_{metal} \\ c_{metal} = \left(m_{Zr} c_{Zr} + m_{Fe} c_{Fe} \right) / m_{metal} \end{cases} \tag{9}$$

The calculate process of the thickness and the side area of the metal layers is shown as follows.

$$l_{metal} = m_{metal} / \rho_{metal} / \left[\pi \left(R_{APG} + l_{abm} \right)^2 \right] \tag{10}$$

$$A_{metal} = 2\pi l_{metal} \left(R_{APG} + l_{abm} \right) \tag{11}$$

In additional, the mass of concrete ablation caused by the metal layer interaction is,

$$m_{conm} = \rho_{con} A_{metal} l_{abm} \tag{12}$$

(3) heat and mass transfer calculation in the oxide layers

As referred in above, the 5th, 6th and 7th layers of the ablation package group consists of oxide ZrO_2, UO_2 and the oxide product of the concrete ablation. Therefore, the heat physical properties of oxide layers can be determined as follows.

$$\begin{cases} m_{oxid} = m_{ZrO_2} + m_{UO_2} + m_{conox} \\ \rho_{oxid} = \left(m_{ZrO_2}\rho_{ZrO_2} + m_{UO_2}\rho_{UO_2} + m_{conox}\rho_{conox} \right) / m_{oxid} \\ \lambda_{oxid} = 10\left(m_{ZrO_2}\lambda_{ZrO_2} + m_{UO_2}\lambda_{UO_2} + m_{conox}\lambda_{conox} \right) / m_{oxid} \\ c_{oxid} = \left(m_{ZrO_2}c_{ZrO_2} + m_{UO_2}c_{UO_2} + m_{conox}c_{conox} \right) / m_{oxid} \end{cases} \quad (13)$$

Thus, the thickness and side area of oxide layer are,

$$l_{oxid} = m_{oxid} / \rho_{oxid} / A_{APG} \quad (14)$$

$$A_{oxid} = 2\pi l_{oxid}\left(R_{APG} + l_{abox} \right) \quad (15)$$

In additional, the mass of concrete ablation caused by the oxide layer interaction can be calculated as follows.

$$m_{conox} = \rho_{con} A_{oxid} l_{abox} \quad (16)$$

2.3 The chemical interaction process calculation

(1) The decomposition process of the concrete

It is well known that the decomposition process of the concrete follows the order of evaporation, dehydration, decomposition and ablation, and it is determined by the temperature of the corium closing to the concrete.

For the concrete which is closed to the oxide layer, the decomposition process of the concrete affected by the temperature of the oxide layer T_{oxid}.

Thus, the following results can be achieved,

If $T_{oxid} \geq T_{evap}$,

Then, $m_{evapox} = \beta_{H_2Oevap} m_{conox}$; (17)

If $T_{oxid} \geq T_{dehy}$,

Then, $m_{dehyox} = \beta_{H_2Odehy} m_{conox}$; (18)

If $T_{oxid} \geq T_{deco}$,

Then, $m_{CO_2ox} = \beta_{CO_2} m_{conox}$; (19)

If $T_{oxid} \geq T_{ab}$, Then, $m_{Feox} = \beta_{Fe} m_{conox}$,

$m_{SiO_2ox} = \beta_{SiO_2} m_{conox}$, $m_{gasox} = \beta_{gas} m_{conox}$. (20)

And the decomposition process of the concrete which is closing to the metal layer is influenced by the temperature of the metal layer T_{metal}.

Thus, the following results can be achieved,

If $T_{metal} \geq T_{evap}$,

Then, $m_{evapm} = \beta_{H_2Oevap} m_{conm}$; (21)

If $T_{metal} \geq T_{dehy}$,

Then, $m_{dehym} = \beta_{H_2Odehy} m_{conm}$;

(22)

If $T_{metal} \geq T_{deco}$,

Then, $m_{CO_2m} = \beta_{CO_2} m_{conm}$; (23)

If $T_{metal} \geq T_{ab}$, Then, $m_{Fem} = \beta_{Fe} m_{conm}$,

$m_{SiO_2m} = \beta_{SiO_2} m_{conm}$, $m_{gasm} = \beta_{gas} m_{conn}$ (24)

In addition, the decomposition process between the concrete closing to the bottom of corium group is influenced by the temperature of the ablation layer T_{bot}.

If $T_{bot} \geq T_{evap}$,

Then, $m_{evapb} = \beta_{H_2Oevap} m_{conb}$; (25)

If $T_{bot} \geq T_{dehy}$,

Then, $m_{dehyb} = \beta_{H_2Odehy} m_{conb}$; (26)

If $T_{bot} \geq T_{deco}$,

Then, $m_{CO_2b} = \beta_{CO_2} m_{conb}$; (27)

If $T_{bot} \geq T_{betab}$, Then, $m_{Feb} = \beta_{Fe} m_{conab}$,

$m_{SiO_2b} = \beta_{SiO_2} m_{conab}$, $m_{gasb} = \beta_{gas} m_{conl}$. (28)

in which,

β_{H_2Oevap} is the mass fraction of the evaporation water in the concrete;

β_{H_2Odehy} is the mass fraction of the dehydration water in the concrete;

β_{C_2O} is the mass fraction of the chemical decomposition CO_2 in the concrete;

β_{Fe} is the mass fraction of Fe in the concrete;

β_{SiO_2} is the mass fraction of SiO_2 in the concrete;

β_{gas} is the mass fraction of the chemical decomposition gas except CO_2 in the concrete.

Thus, the total product of the concrete decomposition can be achieved as follows,

$$\begin{cases} m_{evapab} = m_{evapox} + m_{evapm} + m_{evapb} \\ m_{dehyab} = m_{dehyox} + m_{dehym} + m_{dehyb} \\ m_{CO_2ab} = m_{CO_2ox} + m_{CO_2m} + m_{CO_2b} \\ m_{Feab} = m_{Feox} + m_{Fem} + m_{Feb} \\ m_{SiO_2ab} = m_{SiO_2 2ox} + m_{SiO_2m} + m_{SiO_2b} \\ m_{gasab} = m_{gasox} + m_{gasm} + m_{gasb} \end{cases} \quad (29)$$

(2) The oxygen interaction between the metal and the concrete

The oxide interaction of Zr includes the interaction with H_2O, CO_2 and SiO_2, and the priority is H_2O、CO_2、SiO_2.

$$\begin{cases} m_{ZrH_2O} = \dfrac{(m_{evapab} + m_{dehyab})M_{Zr}}{2M_{H_2O}}, m_{corZr} > 0 \\ m_{ZrCO_2} = \dfrac{m_{CO_2ab}M_{Zr}}{M_{CO_2}}, m_{corZr} - m_{ZrH_2O} > 0 \\ m_{ZrSiO_2} = \dfrac{m_{SiO_2ab}M_{Zr}}{M_{SiO_2}}, m_{corZr} - m_{ZrH_2O} - m_{ZrCO_2} > 0 \end{cases} \quad (30)$$

Thus, the total mass of Zr which was oxidized is,

$$m_{Zrchem} = m_{ZrH_2O} + m_{ZrCO_2} + m_{ZrSiO_2} \quad (31)$$

And for the oxidation interaction of Fe, the first is the interaction with H_2O, and then follows the interaction between Fe and CO_2.

Thus, the masses of oxide Fe which interacted with water and CO2 are,

$$\begin{cases} m_{FeH_2O} = \dfrac{(m_{evap} + m_{dehy})M_{Fe}}{M_{H_2O}}, m_{corFe} > 0 \\ m_{FeCO_2} = \dfrac{m_{CO_2}M_{Fe}}{M_{CO_2}}, m_{corFe} - m_{FeH_2O} > 0 \end{cases} \quad (32)$$

Then, the total mass of oxidation Fe is,

$$m_{Fechem} = m_{FeH_2O} + m_{FeCO_2} \quad (33)$$

And the energy released by the oxide interaction can be calculated as follows,

$$\begin{cases} Q_{ZrH_2O} = m_{ZrH_2O}\left[7.76\times10^6 + 1150(T_{APG4} - 2000)\right] \\ Q_{ZrCO_2} = 5.9\times10^6 m_{ZrCO_2} \\ Q_{ZrSiO_2} = 2.1\times10^6 m_{ZrSiO_2} \\ Q_{FeH_2O} = m_{FeH_2O}\left[5.67\times10^4 + 2241(T_{APG4} - 2000)\right] \\ Q_{FeCO_2} = m_{FeCO_2}\left[3.77\times10^5 + 27.1(T_{APG4} - 2000)\right] \end{cases} \quad (34)$$

Then, the total energy released by the chemical interaction is,

$$Q_{chem} = Q_{ZrH_2O} + Q_{ZrCO_2} + Q_{ZrSiO_2} + Q_{FeH_2O} + Q_{FeCO_2} \quad (35)$$

2.4 The energy conservation

Due to the relative velocity between different layers in the corium group can be neglected, the heat conduction is predominant energy transmission mechanism. Therefore, the heat conduction can be calculated as follows,

$$\begin{cases} Q_{23} = \lambda_{matel} A_{APG} \dfrac{T_{APG2} - T_{APG3}}{l_{APG2}} \\ Q_{34} = \lambda_{matel} A_{APG} \dfrac{T_{APG3} - T_{APG4}}{l_{APG4}} \\ Q_{45} = A_{APG}\left(T_{APG4} - T_{APG5}\right) / \left(\dfrac{l_{APG4}}{2\lambda_{matel}} + \dfrac{l_{APG5}}{2\lambda_{oxid}}\right) \\ Q_{56} = \lambda_{oxid} A_{APG} \dfrac{T_{APG5} - T_{APG6}}{l_{APG5}} \\ Q_{67} = \lambda_{oxid} A_{APG} \dfrac{T_{APG6} - T_{APG7}}{l_{APG7}} \end{cases} \quad (36)$$

And the energy release from the concrete ablation add to the metal and oxide layers can be showing as follows, [shown as Eq. (37)]

$$\begin{cases} Q_{addm} = m_{Feab}c_{Fe}T_{ab} - m_{Fechem}c_{Fe}T_{APG3} - m_{Zrchem}c_{Zr}T_{APG3} + (m_{evap}T_{evap} + m_{dehy}T_{dehy})c_{H_2O} \\ -m_{H_2ab}c_{H_2}T_{APG3} + m_{CO_2ab}c_{CO_2}T_{APG3} - m_{CO}c_{CO}T_{APG3} \\ Q_{addox} = m_{Fechem}\dfrac{M_{feo}}{M_{fe}}c_{Feo}T_{APG3} + m_{ZrO_2chem}c_{ZrO_2}T_{APG3} + m_{gasab}c_{gas}T_{ab} \end{cases} \quad (37)$$

Thus, the energy releasing from the concrete ablation add to each layer can be calculated as following equations.

$$\begin{cases} Q_{iadd} = \beta_i Q_{addm}, i = 2,3,4 \\ Q_{iadd} = \beta_i Q_{addox}, i = 5,6,7 \end{cases} \quad (38)$$

Due to the relative velocity between the corium and the concrete cannot be neglected, the convective heat transfer is predominant energy transmission mechanism. Therefore, the convective heat transfer can be calculated as follows,

$$\begin{cases} Q_{corconi} = h_{metal} A_{metal} \beta_i (T_{APGi} - T_{conab}), i = 2,3,4 \\ Q_{corconi} = h_{oxid} A_{oxid} \beta_i (T_{APGi} - T_{conab}), i = 5,6,7 \\ Q_{corconi} = h_{oxid} A_{APG} (T_{APG7} - T_{conab}), i = 8 \end{cases} \quad (39)$$

And the temperature of layers of the ablation package group can be calculated by the energy balance. Because of the difference of the heat exchange mechanistic among the metal layer, oxide layer and ablation layer, the calculation correlations have been given respectively as follows: [shown as Eq. (40)]

$$\begin{cases} T_{APGi} = \left[T_{efi} c_{metal} m_{APGi} + Q_{addi} + \beta_{APGi} Q_{chem} - (Q_{i,i-1} + Q_{i,i+1} + Q_{corconi}) \Delta t \right] \\ / \left[m_{APGi} c_{metal} + \beta_i \left(m_{Feab} c_{Fe} - m_{Fechem} c_{Fe} - m_{Zrchem} c_{Zr} \right) \right], i = 2,3,4 \\ T_{APGi} = \left[T_{efi} c_{oxid} m_{APGi} + Q_{addi} + (Q_{pi} + Q_{i,i-1} - Q_{i,i+1} - Q_{corconi}) \Delta t \right] \\ / \left[m_{APGi} c_{oxid} + \beta_i \left(m_{Fechem} \frac{M_{FeO}}{M_{Fe}} c_{FeO} + m_{ZrO_2 chem} c_{ZrO_2} + m_{gasab} c_{gas} \right) \right], i = 5,6,7 \\ T_{APGi} = T_{APGi} + \frac{Q_{corcon} \Delta t}{m_{APGi} c_{conab}}, i = 8 \end{cases} \quad (40)$$

2.5 The mass conservation

According to the mass conservation, the mass of each layer of the corium group can be calculated as follows,

$$\begin{cases} m_{APGi} = \beta_i \left(m_{Zr} + m_{Fe} \right), i = 2,3,4 \\ m_{APGi} = m_{APGi} + \beta_i \left(m_{abox} + m_{Fechem} \frac{M_{FeO}}{M_{Fe}} + m_{ZrO_2} \right) i = 5,6,7 \end{cases} \quad (41)$$

And the gas release mass is,

$$\begin{cases} m_{H_2O(out)} = m_{evap} + m_{dehy} - m_{H_2OZr} - m_{H_2OFe} \\ m_{CO_2(out)} = m_{CO_2 ab} - m_{CO_2 Zr} - m_{CO_2 Fe} \\ m_{H_2(out)} = m_{H_2 Zr} - m_{H_2 Fe} \\ m_{CO(out)} = m_{COZr} - m_{COFe} \end{cases} \quad (42)$$

Thus, the ablation rate of the concrete can be calculated as the following equations,

If $T_{APG8} > T_{ab}$, then, $l_{ab} = l_{ab} + \Delta l$; (43)

If $T_{APG8\,ox} > T_{ab}$, then, $l_{abox} = l_{abox} + \Delta l$; (44)

If $T_{APG8\,m} > T_{ab}$, then, $l_{abm} = l_{abm} + \Delta l$. (45)

2.6 Primary parameters of SimSA code

The model that governs the whole MCCI process has been developed, the next step is to solve these equations and create the simulation procedure. The MCCI model solution process as follows: (shown as Fig. 2)

3 Model assessment

The validation of the MCCI model includes the collection of calculation input data, the Daya-Bay 900MWe nuclear power plant is selected as the research object. Using this procedure to calculate the process of the MCCI when the SBO or LOCA severe accident serial is happened and the simulation results is analyzed. The calculation results of this procedure are compared with the large-scale analysis programs MAAP to verify the reasonableness and correctness of the model.

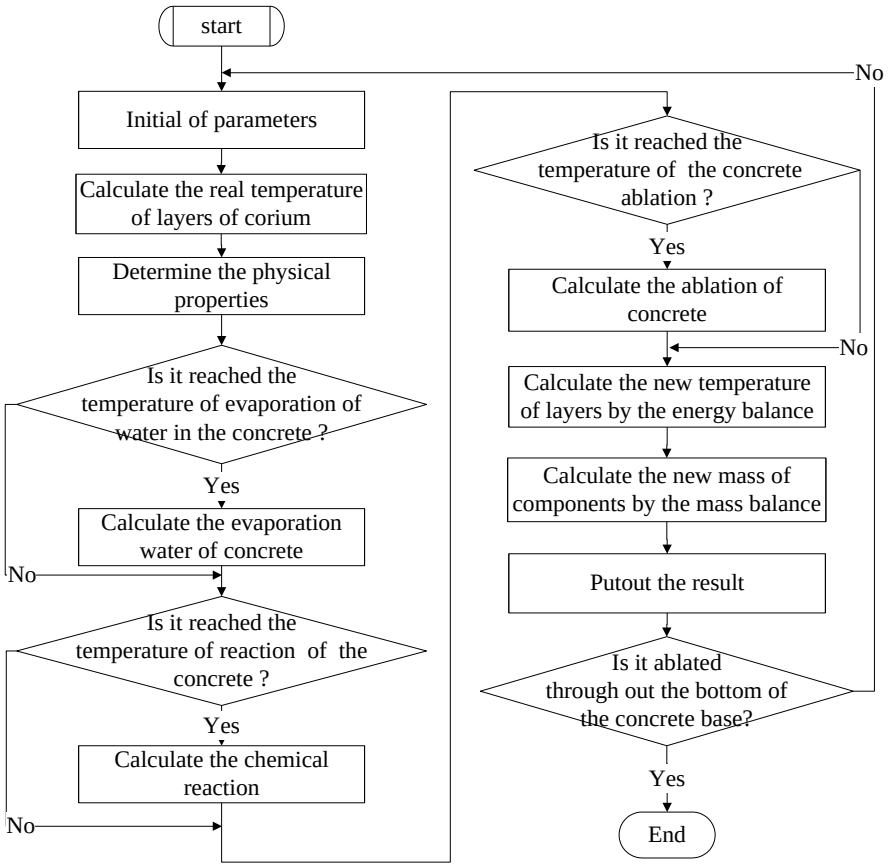

Fig. 2. The calculation fellow of the simulation code.

3.1 Input parameters of model

Cavity geometry and concrete component of Daya-Bay 900MWe nuclear power plant is shown in the Table 1 as following.

The sources term of core corium from the reactor pressure vessel (RPV) can calculated by the MAAP. After the rupture of the RPV, the reactor core melt completely released into the reactor cavity that could be treated as an input source term to the containment. The source term parameters mainly included the initial amount of oxide molten corium, initial amount of metal molten corium, the molten corium initial temperature, the initial temperature of cavity wall surface and the decay power of the corium, *etc.*

Because numerous severe accident sequences could lead to MCCI severe accident process, it is unpractical and unnecessary to calculate all the postulated conditions, and typical accident sequences should be screened out. The large break loss-of-coolant accident (LB-LOCA) and the station blackout (SBO) were selected as typical accident sequences, and the key parameters and boundary conditions of the two accident sequences are shown in Table 2.

Table 1 The Cavity Geometry and Concrete Component of Daya-Bay 900MWe NPP

Parameters	Value/m	Concrete component	Mass fraction/%
Thickness of concrete base	5.5	Si02	0.562
Height of the cavity	10.68	CaO, FeO	0.066,0.135
Radius of the cavity	2.6	Al2O3	0.173
Thickness of the cavity side wall	1.8	CO2,H2O	0.012,0.052

Table 2 Key Parameters and Boundary Conditions for SBO and LBLOCA Sequences Calculation

Initial melt parameters	SBO	LOCA
Mass inventory of the oxide corium/kg	$U0_2$, 80901	$U0_2$, 71661
	$Zr0_2$, 24252	$Zr0_2$, 21463
Mass inventory of the metal corium/kg	Fe, 1649.7; Cr, 120.64	Fe, 1459.72; Cr, 106.7
	N, 53.07 ; Zr,778.93	N, 46.97; Zr, 689.35
Temperature of the corium/K	T_m, 1784; T_o, 2804	T_m, 1875; T_o, 2943
	T_{avg}, 2774	T_{avg}, 2848
Temperature of the concrete/K	714	368
Decay heat (the zero time is reactor trip)	1.3E4s, 235; 2.6E4s, 186; 4E4s, 167; 9E4s, 136; 1.9 E5s, 96; 1.34E6s, 48	

3.2 Results and discussions

(1) The calculation results of LBLOCA accident sequence

In other to verify the exactness of the models, the MCCI process under the LBLOCA with the safety injection fail severe accident sequence has been calculated respectively by the SimSA code and MAAP, and the difference between SimSA and MAAP results of the key parameters are shown in the Fig. 3.

The total mass and the temperature of corium group, the ablation depth of concrete, the mass of hydrogen produced in the accident have been selected and checked.

From Fig. 3(a)&(b) above, the corium group mass and temperature calculated by SimSA is mostly higher than the MAAP result in the beginning and the interim. The difference comes from the new hierarchical structures applied in MCCI models. It changes the heat and mass transfer calculation in the oxide layers, leads the fuel rods melting earlier. Due to the corium group structures considering the ratio of metal layer reasonably, and also calculating the interaction process between the liquid metal layer and the oxide layer, the first peak mass and temperature are both lower than MAAP values. However, the global trends are similar, and the result of SimSA achieves greatly close with the value of MAAP. All those above evidences support the correctness of MCCI.

In Fig. 3(c), the almost identical values and trends in the whole period support the accuracy of MCCI models. According to the decomposition process models, the concrete ablation depth depends on the temperature distribution around the different layer interfaces. The concrete zone locates in the bottom, covering with the ablation oxide production layer and partly separated with the metal oxide layers. Therefore, the ablation process is not sensitive to the upper layer components type.

(2) The calculation results of SBO accident sequence

The MCCI process under the SBO with loss of auxiliary feed water severe accident sequence has been calculated respectively by the SimSA code and MAAP, and the difference between SimSA and MAAP results of the key parameters are shown in the Fig. 4.

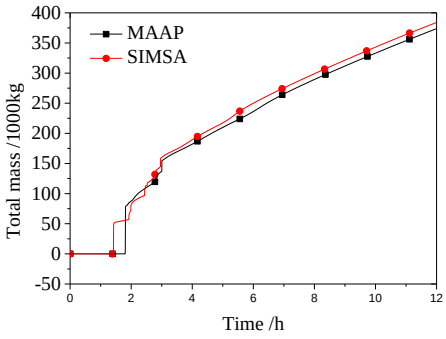

a. The total mass of corium group

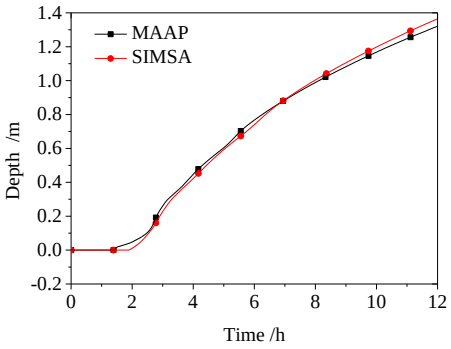

c. The ablation depth of concrete

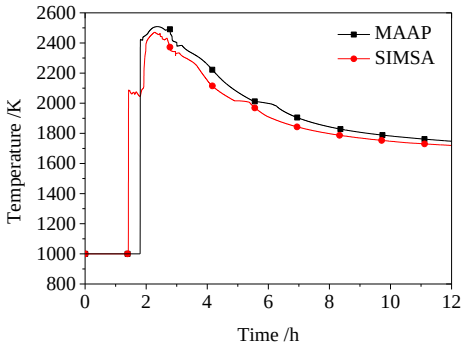

b. The temperature of corium group

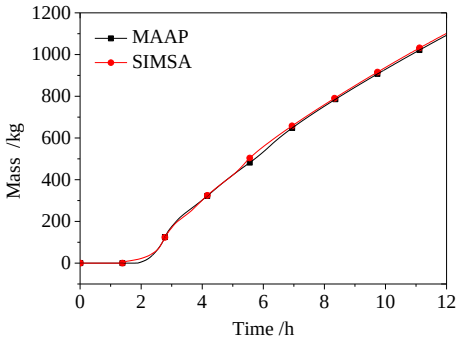

d. The mass of hydrogen produced by MCCI

Fig. 3. MCCI calculation comparison between MAAP and SimSA code of LBLOCA sequences.

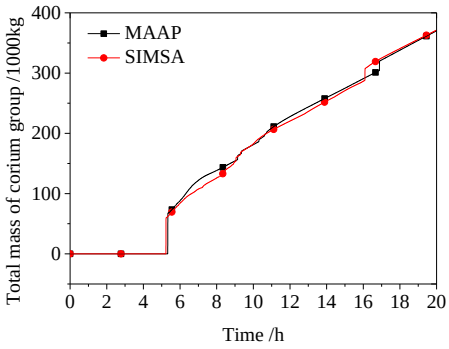

a. The total mass of corium group

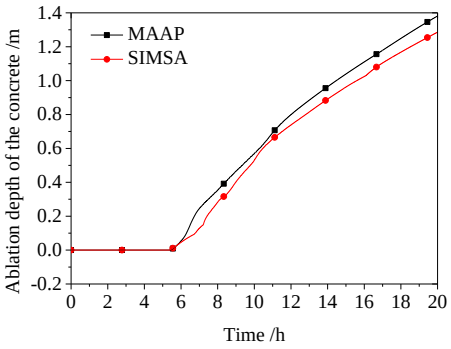

c. The ablation depth of concrete

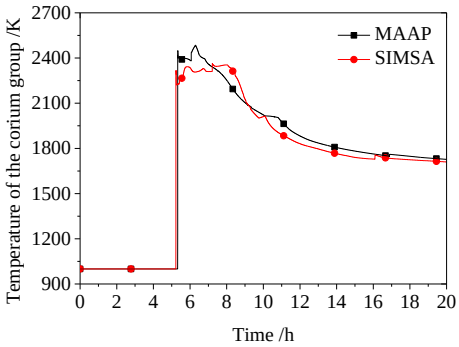

b. The temperature of corium group

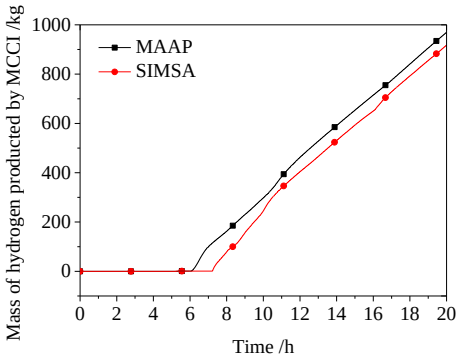

d. The mass of hydrogen produced by MCCI

Fig. 4. MCCI calculation comparison between MAAP and SimSA code of SBO sequences.

(3) Result analysis

From the results listing above, we can find that the SIMSA calculation results are in a good agreement with MAAP code, and there is also some small difference in the temperature of the corium group, the result of MAAP is higher than SIMSA. And it leads to the concrete ablation depth and hydrogen generation calculated by MAAP is bigger than SIMSA.

The convective heat transfer between the water film and the corium group is a major mitigation measure of MCCI process, with plenty water evaporation much decay heat was removed away from the molten corium group. Generally, a solid shell will be formed in the surface of the corium group, and this shell will reduce the efficiency of the convective heat transfers between the water film and corium group in a certain degree. This phenomenon has been considered in the MAAP model but not exited in SIMSA, and this is why the temperature of corium group calculated by MAAP is higher than SIMSA.

And due to using the same two layer hierarchical structure of the molten corium group, the SIMSA calculation results agree well with MAAP code. But to meet the real time requirement of simulator in every time step under all transient state, SIMSA did not consider some detail process such as the impact of solid shell to heat transfer and so on. This improvement raise the calculation speed and also loss some precision, but this loss of precision is acceptable.

4 Conclusions

In the present study, a new mechanistic model of MCCI process under severe accidents is developed and verified to meet the fast calculation need of FSS. The hypotheses accident sequences of SBO and LBLOCA in DAYA-Bay nuclear power plant is selected as the research objection. And the analyses results of the new developed model and MAAP are compared indirectly.

The results show that the main parameters of MCCI process, such as concrete ablation depth, ablation group temperature and hydrogen generation, are basically consistent between the new model and MAAP. It indicated that the precision of the procedure is closed to the MAAP.

Nomenclature

D_e hydraulic equivalent diameter (m)

H enthalpy (J/kg)

K resistance coefficient

P pressure (MPa)

m_{zrh2o} mass of zirconium consumed in reaction

m_{h2ozr} mass of water consumed in reaction

m_{h2zr} mass of hydrogen generated in reaction

m_{beti} mass of i-th layer corium

m_{feabi} mass of i-th layer corium Fe addition

$m_{fechemi}$ mass of i-th layer corium Fe reduced

$m_{zro2chemi}$ mass of ZrO_2 generated in reaction

m_{gasabi} mass of i-th layer corium gas adddition from ablation

M_{zr} mole mass of zirconium atom

M_{h2o} mole mass of the water molecule

M_{h2} mole mass of hydrogen molecule

M_{feo} mole mass of FeO

M_{fe} mole mass of metal Fe

T_{efi} temperature of layers of the ablation package group

Q_{addi} i-th layer corium energy addition brought by the ablation of concrete,

Q_{pi} i-th layer corium decay heat

$Q_{i,i\pm1}$ energy of thermal conduction from adjacent two layers

$Q_{corconi}$ convection heat transfer from ablation layer

Q_{chemi} energy of metal oxidation reaction

c_{metal} heat capacity of metal layers

c_{oxid} heat capacity of oxid layers,

c_{fe} heat capacity of metal Fe

c_{zr} heat capacity of metal Zr

c_{zro2} heat capacity of Zr O_2

c_{feo} heat capacity of FeO

c_{betox} heat capacity of concrete

Δt time step

α vapor volume fraction

υ kinematic viscosity (m^2/s)

Subscripts

in inlet

out outlet

References

[1] MERRILL, B.J., HUMRICKHOUSE, P.W., and MOORE, R.L.: A recent version of MELCOR for fusion safety applications. Fusion Eng. Des. 85 (7e9), 1479-1483, 2010.

[2] NNSA: Nuclear power plant operation safety regulations of national nuclear safety regulatory authorities of China (NNSA), HAF103. Chapter 3.12, 9-14. 2004.

[3] FERNG, Y.M., LIU, Y.T., and SHIH, C.: Investigating Exec. EOPs LOTDFP + ATWS + LOCA scenarios for an ABWR using MAAP code 240 (1), 198-203, 2010.

[4] SHARMA, B.M., TIWARI, A., SRIVASTAVA, A., KUMAR, R., LELE, H.G., and KHANNA, A., *et al.:* Analysis of PHWR LP turbine steady state using RELAP/SCDAP code. Energy Procedia 7, 367-373, 2011.

[5] CARROLL, D.E., TILLS, J.L., VALDEZ, G.D., BERGERON, K.D., and WILLIAMS, D.C.: Integrated analysis of core debris interactions and their effects on containment integrity using the contain computer code. Nucl. Eng. Des. 104 (3), 277-283, 1987.

[6] MAKYNEN, J.M., JOKINIEMI, J.K., and KAUPPINEN, E.I.: LWR aerosol experiments at Victoria model containment. J. Aerosol Sci. 28 (1), s715es716, 1997.

[7] BANDINI, G., MELONI, P., POLIDORI, M., and LOMBARDO, C.: Validation of CATHARE V2.5 thermal-hydraulic code against full-scale PERSEO tests for decay heat removal in LWRs. Nucl. Eng. Des. 241 (12), 4662e4671, 2011.

[8] TOURNIAIRE, B.: A heat transfer correlation based on a surface renewal model for molten core concrete interaction study. Nuclear Engineering and Design, 2006. 236(1): p. 10-18.

[9] CNPO: User's Manul of Simulation code of Severe Accident (SimSA), Internal document CNP/SEC/A110610/RP/0003 of CNPO, 7-9, 2014.

[10] WEI, W., QI, K.L., SHAN, F.C., CHEN, Y.F., and GUO, F.D.: The development of a mechanistic model of MCCI under severe accidents. In: ICONE21, Chendu, China, July 21eAugust 2, 2013.